Frontiers in Bioscience Landmark

Front. Biosci. (Landmark Ed) **2023**; 28(3): 52
https://doi.org/10.31083/j.fbl2803052

Original Research

PARP Inhibition Sensitizes Breast Cancer Cells to Eribulin

Bahram Sharif-Askari[1], Lawrence Panasci[1,*], Raquel Aloyz[1]

[1]Montreal Centre for Experimental Therapeutics in Cancer Segal Cancer Center, Lady Davis Institute for Medical Research, Jewish General Hospital, McGill University, Montréal, QC H3T 1E2, Canada

*Correspondence: Lawrence.panasci@mcgill.ca (Lawrence Panasci)

Academic Editor: Alfonso Urbanucci

Submitted: 17 October 2022 Revised: 2 March 2023 Accepted: 6 March 2023 Published: 16 March 2023

Abstract

Background: Poly(ADP-ribose) polymerases 1 and 2 (PARP1, 2), and 3 mediate protein modifications that facilitate the recruitment of DNA repair factors to single and double strand breaks. PARP3 is unique in that it is also required for efficient mitotic progression and stabilization of the mitotic spindle. Eribulin, an anti-microtubule agent used clinically to treat breast cancer, exerts its cytotoxicity by altering microtubule dynamics resulting in cell cycle arrest and apoptosis. Herein, we hypothesize that the pan PARP inhibitor olaparib has the potential to enhance the cytotoxicity of eribulin by halting mitosis through inhibition of PARP3. **Methods**: The effect of olaparib on eribulin cytotoxicity was assessed using the Sulforhodamine (SRB) assay, with two triple negative breast cancer cell lines and an estrogen receptor positive (ER+)/human epidermal growth factor receptor 2 negative (HER2-) breast cancer cell line. Alteration by the treatments on PARP3 activity and microtubule dynamics were assessed utilizing a chemiluminescent enzymatic assay and immunofluorescence, respectively. The effect of the treatments on cell cycle progression and apoptosis induction were assessed by flow cytometry using propidium iodide and Annexin V staining, respectively. **Results**: Our results demonstrate that non-cytotoxic concentrations of olaparib sensitize breast cancer cells regardless of ER status. Mechanistically, our results indicate that olaparib potentiates eribulin-induced cell cycle arrest at the G2/M boundary, PARP3 inhibition and microtubule destabilizing resulting in mitotic catastrophe and apoptosis. **Conclusions**: In breast cancer (regardless of ER status) settings, treatment outcomes could be improved by the incorporation of olaparib in eribulin treatment regimens.

Keywords: eribulin; olaparib; PARP3 inhibitor; drug combination; breast cancer cell lines; microtubule dynamics

1. Introduction

The poly (ADP-ribose) polymerase (PARP) superfamily includes 17 members involved in a variety of cellular processes such as transcription, chromatin status regulation, telomere function, and DNA repair [1]. PARPs play an important role in DNA repair because they facilitate the recruiting of DNA repair components to single strand breaks (SSBs) and double strand breaks (DSBs). The observation that deficiencies in PARP and DNA DSB repair processes are synthetically lethal prompted the clinical development of PARP inhibitors to target BRCA1/2 driven cancers. These efforts led to the development of olaparib. Olaparib is an FDA approved pan PARP inhibitor that shows promising effects in breast cancer gene (BRCA) 1/2-deficient breast and ovarian cancer cells plus in BRCA-mutated patients bearing these tumors [2–8]. BRCA1 has a role in the repair of DNA damage, especially cytotoxic double-stranded DNA breaks (DSBs), which are important types of DNA lesions. Homologous Recombinational Repair (HRR) is a critically important mechanism leading to DNA damage correction. BRCA1 is central to several macromolecular complexes and as one of the major tumor suppressor proteins drives HRR and cell cycle progression [9]. HRR proficiency is one of the major determinants of cellular sensitivity to PARP inhibitors because restoring homologous recombination repair limits sensitivity to PARP inhibitors [9–11]. As well, PARP inhibition by olaparib was shown to sensitize tumor cells to DNA-damaging drugs and radiation [8,12,13]. PARP1 is the best characterized family member whose catalytic poly (ADP-ribosyl) ation activity is one of the earliest responses to SSBs and DSBs [14,15]. As well as other PARP family members, PARP3 interacts with both classical and alternative nonhomologous end-joining (NHEJ) proteins herein facilitating DSB repair. PARP3 participating in DSB repair pathway(s) by interact with the classical nonhomologous endjoining (C-NHEJ) proteins, DNA-PK, KU70, KU80, and DNA ligase IV [16]. In contrast, only PARP3 is required for efficient mitotic progression as it stabilizes the mitotic spindle and promotes telomere integrity [16–18]. Although, PARP3 is a core component of the centrosome [19], it appears to regulate cell cycle progression without interfering with centrosome duplication [20]. Even though the mechanistic role of PARP3 in mitotic spindle stabilization is not completely understood, it is plausible that PARP3 inhibitors affect mitotic progression by delaying both DSB repair and spindle assembly [19,21].

Our working hypothesis is that because of its role in mitotic progression, reduction of PARP3 activity has the potential to enhance the efficacy of anticancer agents targeting microtubule dynamics. We previously demonstrated

that in a triple negative breast cancer (TNBC) cell lines, a nontoxic dose of a pan PARP inhibitor (olaparib) or a selective PARP3 inhibitor (ME-0328) leads to enhanced antitumor activity of a vinca alkaloid (vinorelbine) but not a taxane (paclitaxel) [22]. These results suggest that inhibition of PARP3 sensitizes breast cancer cells to anticancer agents that cause dissolution of the mitotic spindle such as vinorelbine but not to taxanes which stabilize the mitotic spindle. In the current work, we examined the effect of olaparib on eribulin cytotoxicity in human breast cancer cell lines [23,24]. Eribulin mesylate is an FDA-approved non-taxane microtubule inhibitor. Eribulin is utilized to treat patients with metastatic breast cancer, especially those bearing the HER2 negative genotype [25–28]. Eribulin inhibition of microtubule dynamics occurs through a novel mechanism of action. In contrast to taxanes that shorten microtubules, eribulin binds to a unique part of tubulin site, leading to suppression of microtubule polymerization with no effect on microtubule depolymerization. Furthermore, eribulin (but not taxanes) can promote the tubulin degradation to nonfunctional aggregates [23,26]. Consequently, eribulin generates fine structural changes of the mitotic spindle which are sufficient to cause cell cycle arrest at the G2-M boundary [25,29] leading to an irreversible block in mitosis and apoptosis [23,26,27]. The effect of olaparib on eribulin cytotoxicity was evaluated in breast cancer cell lines.

2. Materials and Methods

2.1 Cell Lines, Drug Treatments, Reagents

MDA-231 and MDA-436 are triple negative breast cancer cell lines and MCF-7 is an ER+/HER2- breast cancer cell line. They were obtained from the American Type Culture Collection (ATCC) and maintained following the manufacturer instructions. The cell lines used have been tested and are negative for mycoplasma. Eribulin mesylate 0.5 mg/mL was obtained from Eisai LTD (Mississauga, ON, Canada) and olaparib was provided by Selleckchem Company (Houston, Texas, USA).

2.2 Sulforhodamine (SRB) Assay

The SRB cytotoxicity assay in breast cancer cell lines was assessed 5 days after treatment using the SRB colorimetric assay as described by us [30,31]. The IC_{50} of each compound was determined utilizing a range of concentrations; olaparib (0.1–20 μM) and eribulin (1–1000 nM). Breast cancer cells were treated with olaparib and eribulin alone or with drug combinations based on the concentration as indicated in the results section. The efficacy of the various drug treatments was determined by calculating sensitization values (*R*-values) using the equation described by us [32,33]. The experiments were repeated at least three times and each experiment consisted of triplicate drug treatment. In all experiments, wells treated with DMSO (vehicle) and olaparib alone were considered as controls.

2.3 Apoptosis Assay

Apoptotic cell death levels were assessed by monitoring drug-treated cultures for Annexin V content using flow cytometry as described by us [34]. After 24 hours, the breast cancer cells treated with the stated drug combinations and concentrations were assayed by using the PE Annexin V Apoptosis Detection Kit (BD Pharmingen, Waltham, MA, USA) as previously described [22].

2.4 Cell Cycle Assay

Breast cancer cell lines were grown in T25 flasks including Roswell Park Memorial Institute culture media (RPMI) and 10% Fetal Bovine Serum (FBS), and then treated with olaparib and eribulin alone and drug combinations for 24 hours as described [22]. Cell cycle analysis was performed using a BD Fortessa flow cytometer (BD Biosciences, San Jose, CA, USA) flow cytometry [30,32]. A minimum of 20,000 events was recorded for each sample.

2.5 PARP Inhibition Assay

Breast cancer cell lines (5×10^5 cells) were grown in T25 flasks for 24 hours as described [30]. The resulting supernatant was assayed for PARP activity using the PARP3 chemiluminescent assay kit (BPS bioscience, San Diego, CA, United States) as described by us [22].

2.6 Visualization of Altered Microtubule Networks

To assess alterations in microtubule networks that associated with the microtubule depolymerization effects the breast cancer cells were seeded, treated and immunostained for tubulin in multichamber slides 24 hours after treatment as indicated [35–37]. Briefly, after treatment, the cells were fixed and permeabilized using 4% formaldehyde for 15 min at room temperature, followed by washing with PBS/BSA for 5 min three times. Then the cells were incubated in PBS/BSA (5%)/Triton X100 (0.1%) for 30 minutes at room temperature. Next, the cells were incubated overnight at 4 °C with α-Tubulin (DM1A) Mouse mAb (Alexa Fluor 488 conjugate) (1:100 dilution in PBS containing 0.1% BSA). After washing the cells with PBS/BSA for 5 min three times, the cells were stained with 4,6-diamidino-2-phenylindole (DAPI; Sigma, St. Louis, MO, USA) (1 μg/mL final solution in PBS) for 5 minutes at room temperature followed by mounting in prolong gold. Fluorescence images were obtained using an (Widefield Leica DM LB2) upright fluorescence microscope with a 40× and 100× objectives (green fluorescence, FITC; and blue fluorescence, DAPI). ImageJ software (Version 1.53t 24, National Institutes of Health, Bethesda, MD, USA) was used for image processing [22].

Cells showing abnormal α-tubulin staining or nuclear morphology were quantified as described [38]. Briefly, manual counts of the obtained images were then processed using the ImageJ software. Preceding manual counting, im-

ages were cropped, scaled to μm and separated by color channel, and artifacts were removed. The ImageJ cell counter tool recorded mouse clicks on cells that were labeled with colored dots [38]. The frequency of abnormal nucleus for each treatment was obtained by dividing the number of abnormal looking cells (size and shape) by the total cell number in the field. These abnormalities are revealed by the morphology of DAPI staining which can be used to identify alteration shape, size, chromatin condensation and giant or multinucleated cells.

2.7 Statistical Analysis

The experiments were performed in triplicate. Analysis of variance and two-sided or paired *t*-test were performed using Sigma Plot Version 13.0 Systat. Software, Inc., San Jose, California, CA, USA. Differences were considered significant with p values < 0.05.

3. Results

3.1 Olaparib Sensitizes Breast Cancer Cells to Eribulin

The cytotoxicity of olaparib and eribulin were determined using the SRB assay to obtain the IC_{50} of the drugs in MDA-231, MDA-436 and MCF-7 cells. The IC_{50} is defined as the concentration of drug that results in a 50% reduction in cell number with respect to vehicle treatment (control). The IC_{50} values were determined utilizing a range of concentrations of olaparib (0.1–20 μM) or eribulin (0.03–300 nM) for the 3 cell lines tested. The IC_{50} of eribulin was in the nanomolar range (1.46, 4.36, and 5.60 for MCF-7, MDA-231A M and MDA-436, respectively) (**Supplementary Fig. 1A–C**). Olaparib IC_{50} was in the μM range for all 3 cell lines. The effect of olaparib on eribulin cytotoxicity was tested by combining olaparib at a non-cytotoxic concentration (2 μM) with a dose range of eribulin (0.03–300 nM). Olaparib enhances eribulin cytotoxicity in all 3 breast cancer cell lines tested with significantly different sensitization by 3-fold in MCF-7 cells, 5-fold in MDA-231 and 8.6-fold in MDA-436 cells, respectively (Fig. 1A–D). Our results indicate that olaparib at a nontoxic concentration (2 μM) sensitized two TNBC cell lines (MDA-231 and MDA-436) and one ER+/HER2- breast cancer cell line, MCF-7 to eribulin. Furthermore, the reduced of eribulin IC_{50} by olaparib was significantly more pronounced in the two TNBC cell lines with respect to MCF-7 cells.

3.2 Olaparib Enhances Eribulin-Induced G2/M Cell Cycle Arrest, Apoptosis and Reduction of PARP-3 Activity

We next assessed the contribution of programmed cell death and cell cycle arrest to the sensitization effect of olaparib on eribulin cytotoxicity. Treatment with eribulin IC_{50} alone (but not Olaparib alone) induces cell cycle arrests in a significant percentage of cells (approx. 50%) in MCF-7 and MDA cells (Fig. 2A–C). Furthermore, cell cycle analysis of MCF-7, MDA-231 and MDA-436 revealed that olaparib enhances significantly eribulin induced cell cycle arrest at the G2/M 24 hours after treatment (Fig. 2A–C). Representative cell cycle profiles and analysis for MDA-231 cell line are shown in **Supplementary Fig. 2**. We next assessed for differences in programmed cell death by monitoring the expression of Annexin V 24 hours after treatment with eribulin IC_{50} and 2 μM olaparib alone or in combination. Olaparib did not significantly affect the percentage of Annexin V in eribulin treated MCF-7 cell nor in MDA-231 cells (data not shown). In MDA-436 cells although the effects were discrete, eribulin IC_{50} alone (but not olaparib alone) increased Annexin V expression, an effect that was enhanced by olaparib (Fig. 3A,B and **Supplementary Fig. 2**).

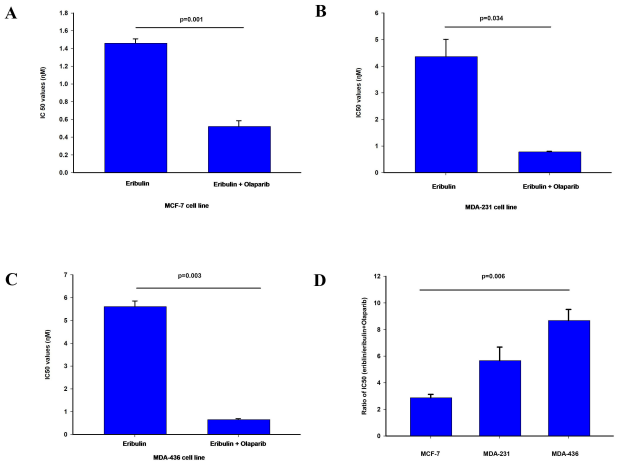

Fig. 1. Effect of olaparib on eribulin cytotoxicity. The IC_{50} values of eribulin alone or in combination with 2 μM of olaparib in one ER+/HER2- breast cancer cell line (A) MCF-7 and two triple negative breast cancer cell lines (B) MDA-231 and (C) MDA-436 cell line is shown. The bars represent the ratio between the IC_{50} of eribulin/IC_{50} of eribulin in combination with 2 μM of olaparib for each cell line. The results are presented as mean $\pm$ standard error (n = 3). Statistical differences were assessed by paired *t*-test (A–C) or Anova (D). Significance is indicated by $p < 0.05$. NS indicates $p > 0.05$.

Because PARP3 activity is required for efficient mitotic progression [16–18], we assessed for changes in PARP3 activity in MDA-436 cells by the drug treatments. The Eribulin IC_{50} concentration or 2 μM olaparib alone both decreased significantly PARP3 activity with respect to vehicle treated cells (CTL) while the combination of the 2 drugs resulted in a further significant decrease in PARP3 activity (Fig. 3C).

In summary, our results show that eribulin induces cell cycle arrest at the G2/M boundary. Furthermore, while our results suggest that olaparib enhanced eribulin-induced cell cycle arrest in all cells, there is a heterogeneous response to the combination of both drugs on apoptosis. This agrees with the reported effect of eribulin on cell cycle progression

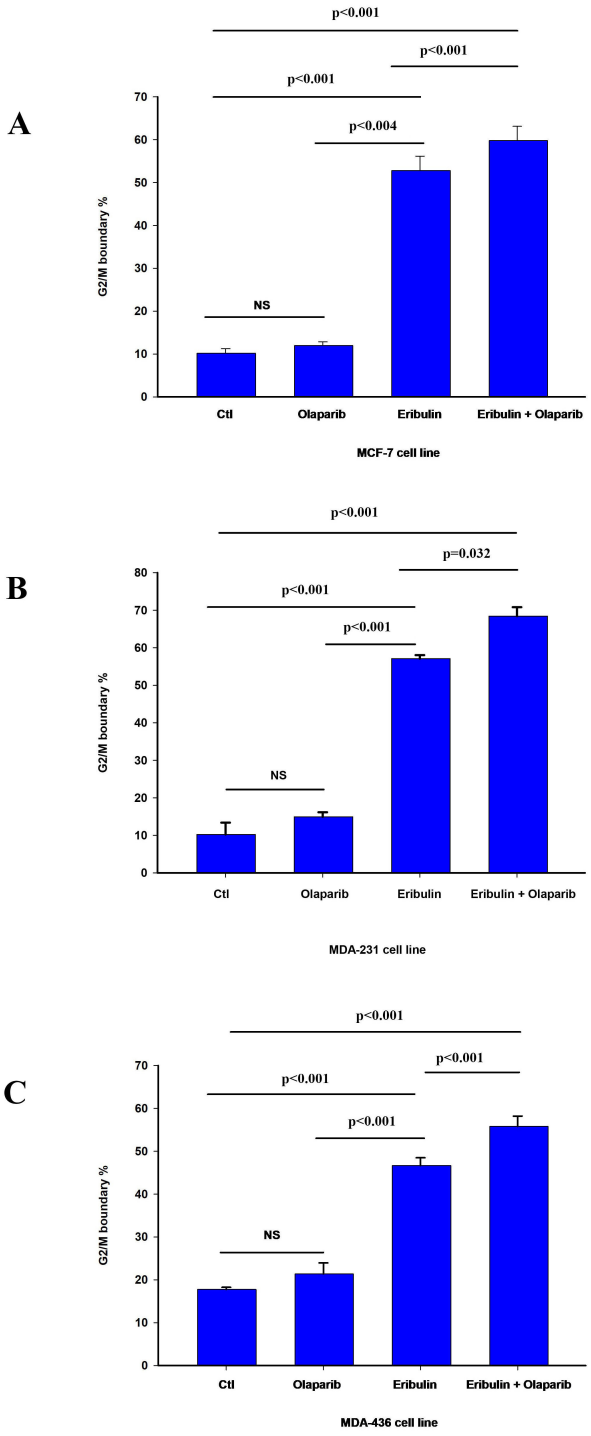

Fig. 2. Effect of olaparib on eribulin-induced G2/M cell cycle arrest. Cell cycle analysis was performed by flow cytometry as described in material and methods. The bar graphs represent the percentage of cells at the G2/M cell cycle boundary in MCF-7 (A), MDA-231 (B), and MDA-436 (C) cell line 24 h after treatment as indicated. The data is presented as the mean value $\pm$ standard error (n = 3). Statistical difference was assessed by Anova followed by *t*-test. Significance is indicated by $p < 0.05$, NS indicates a $p > 0.05$.

and heterogenous induction of programmed cell death [39, 40].

Importantly, 2 μM olaparib alone reduced significantly PARP3 activity without affecting cell number (e.g., SRB assay), apoptosis (Annexin V staining), nor cell cycle progression (e.g., cell cycle arrest). Therefore, it is possible that PARP3 activity contributes to microtubule stabilization and mitotic activity in eribulin treated cells.

3.3 Olaparib Enhanced Eribulin-Induced Nuclear Microtubule Staining and Aberrant Nuclear Morphology

To test the impact of PARP3 activity on microtubule dynamics and markers of mitotic arrest in cells treated with eribulin, we assessed the effect of eribulin and olaparib alone or in combination on tubulin staining and nuclear morphology that have been associated with altered microtubule dynamics by eribulin and other microtubule targeting agents [35–37,41]. MDA-231 and MDA-436 24 hours after treatment with vehicle (CTL), eribulin IC_{50}, 2 μM olaparib or the combination of eribulin plus olaparib. Nuclear microtubule destabilization was estimated as a shift towards enhanced nuclear α-tubulin staining with respect to vehicle-treated CTL cells as described in material and methods. Representative images for MDA-231 and MDA-436 cells are shown respectively in Fig. 4A,B. Altered microtubule dynamics were expressed as the fraction of nucleus showing enhanced depolarization with respect to the total cell numbers for each condition. The results show that eribulin at the IC_{50} concentration (but not 2 μM olaparib) significantly enhanced the frequency of nucleus showing microtubule depolarization with respect to vehicle treated cells in both MDA-231 cells (Fig. 4C) and MDA-436 cells (Fig. 4D). However, 2 μM olaparib increased significantly nuclear microtubule depolarization induced by the eribulin IC_{50} (Fig. 4E).

The effect of olaparib on eribulin microtubule depolarization was significantly more pronounced in MDA-436 cells with respect to MDA-231 cells (Fig. 4E). We observe a similar effect by these treatments in the frequency of cells with abnormally looking nucleus in shape and size such as giant cells shown in Fig. 4 (**Supplementary Fig. 3A,B**).

Overall, our findings suggest that eribulin and olaparib when combined result in greater disruption of microtubule dynamic and altered nuclear morphology than when used alone, effects that have previously been associated with increased chromosome misalignment and splayed microtubule spindles leading to mitotic arrest [23–25,29].

4. Discussion

Targeting PARP by small-molecule inhibitors is a promising anticancer approach to the treatment of metastatic breast cancer [2]. The most studied PARP inhibitors which are currently used in clinical trials are PARP1 and PARP2 inhibitors [15,42,43]. Inhibitors of PARP3, which have a unique function on DSBs repair path-

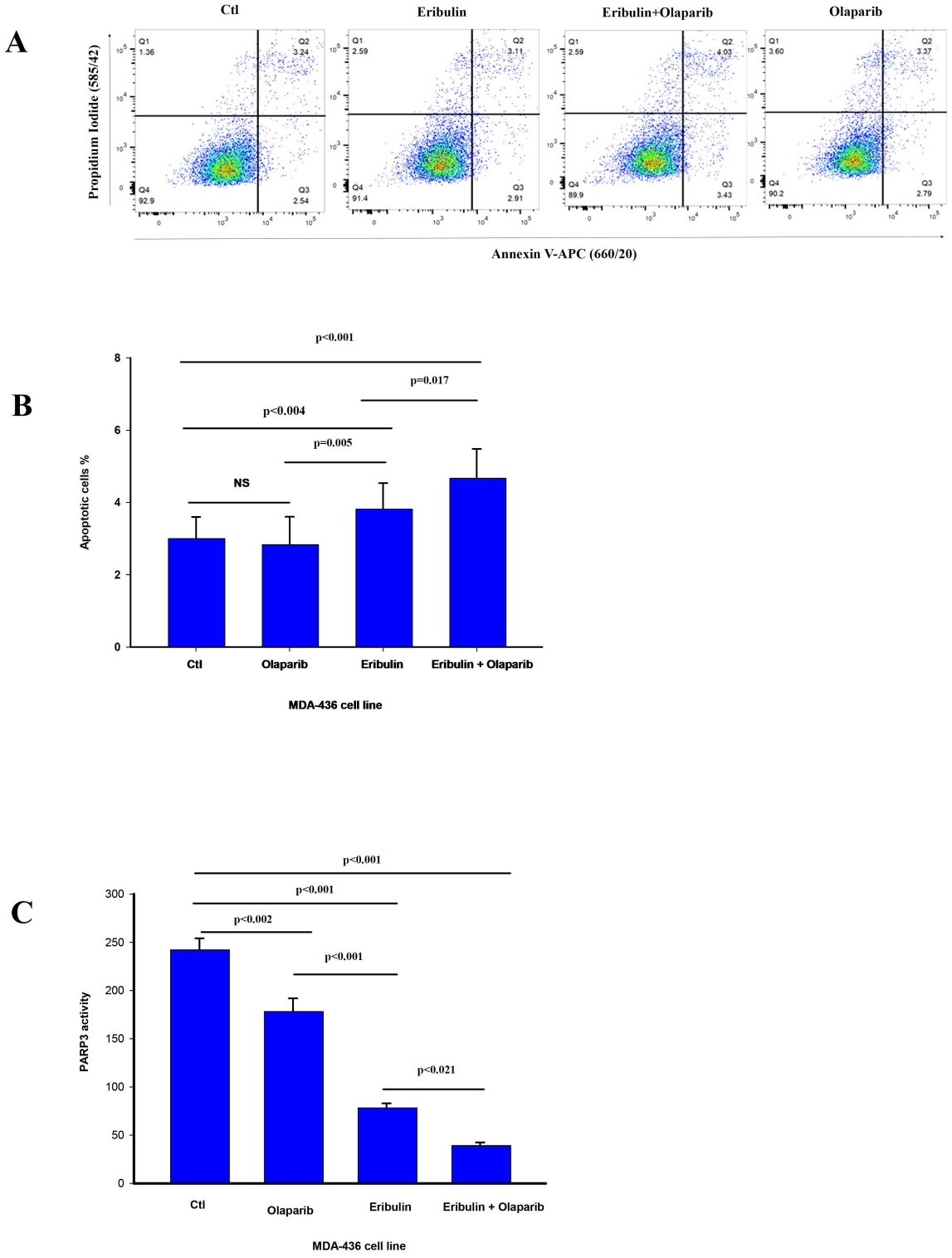

Fig. 3. Olaparib enhances eribulin induced apoptosis and reduces PARP3 activity. (A) The percentage cells undergoing apoptosis was assessed by flow cytometry analysis of Annexin V staining 24 h after treatment with vehicle (CTL) and eribulin IC_{50}, 2 μM of olaparib alone or in combination as indicated. (B) The bars represent the mean value of the percentage of cells undergoing apoptosis after treatment as indicated $\pm$ standard error (n = 3). Statistical differences were assessed by Anova followed by *t*-test. Significance is indicated by $p < 0.05$, NS indicates $p > 0.05$. (C) The effect of olaparib and eribulin on PARP3 activity in MDMA-436 cells was assessed as described in materials and methods 4 h after treatment. The bars represent the mean value $\pm$ standard error (n = 3). Significant differences were assessed by Anova followed by *t*-test. Significance is indicated by $p < 0.05$.

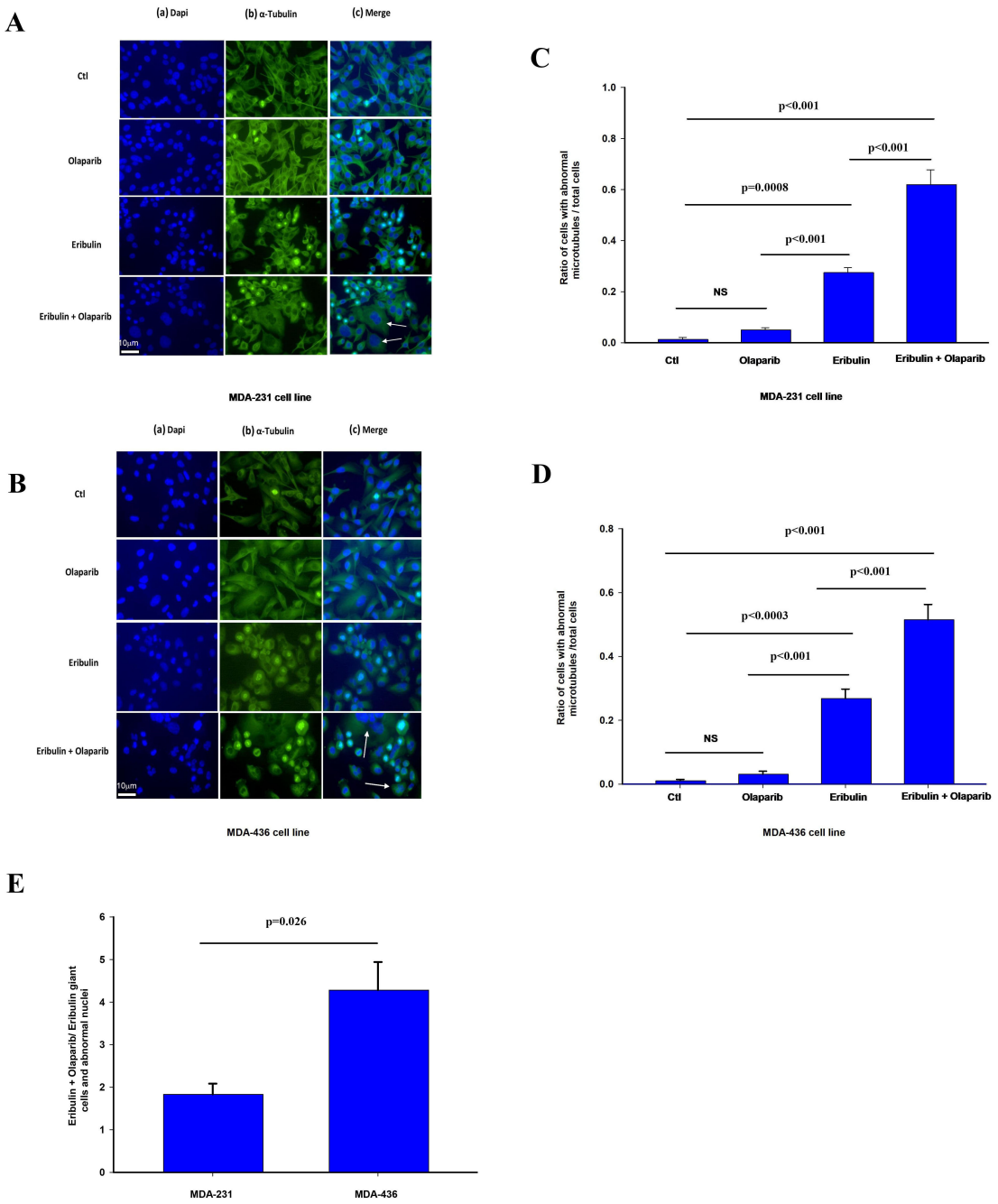

Fig. 4. Effect of olaparib and eribulin on α-tubulin nuclear staining. Panels (A) and (B) show representative immunofluorescent staining for MDA-436 and MDA-231 cells respectively. DNA was stained with DAPI (a) in blue and microtubules with an α-tubulin antibody in green (b). Altered microtubule dynamics is visualized by nuclear α-tubulin staining in merged images (c). The images were acquired 24 h after treatment as indicated with vehicle (CTL), eribulin IC_{50}, 2 μM of olaparib or the combination of eribulin and olaparib. Cells with abnormal multinucleated giant cells are indicated with white arrows. (C,D) The bars represent the mean ratio of cells with abnormal microtubules dynamics in five microscopic fields quantified $\pm$ standard error (n = 3) for MDA-436 (C) and MDA-231 (D). (E) The bars represent the mean values $\pm$ standard error of the ratio between the frequency of cells with abnormal α-tubulin nuclear staining after treatment with eribulin IC_{50} in combination with 2 μM of olaparib/the frequency of cells with abnormal α-tubulin nuclear staining after treatment with eribulin IC_{50} (n = 3). Statistical analysis was performed by Anova followed by *t*-test. Significance is indicated by $p < 0.05$ and NS indicates $p > 0.05$. Cells with abnormal multinucleated giant cells are indicated with white arrows. The pictures were taken with a x40 enlargement.

way and mitotic spindle dynamics have been developed recently [19,21]. Olaparib, although first described as PARP1 and PARP2 inhibitors, has recently demonstrated a critical role in PARP3 inhibition [2,8]. Olaparib, which has been approved by the US Food and Drug Administration (FDA), providing significant advances in the treatment of patients with HER2 negative BRCA mutated metastatic breast cancer [4,5,8,13]. Despite this, resistance of cancer cells to PARP inhibitors has been reported with olaparib like many other anticancer drugs [44]. Moreover, patients with BRCA-mutated tumors represent a small minority of patients.

Eribulin is an FDA-approved non-taxane microtubule inhibitor. Eribulin is utilized to treat patients with metastatic breast cancer, especially those bearing the HER2 negative genotype [25–28]. The antiproliferative mechanisms of eribulin are characterized by suppression of the centromere and changes in spindle microtubule dynamics during mitotic arrest [45]. Eribulin, like other vinca alkaloids, binds to the β-tubulin subunit [23,46]. However, while other vinca alkaloids bind to the end of microtubules and microtubule sides [47], eribulin preferentially binds to the microtubule plus ends, which induces microtubule dynamic instability and spindle microtubule suppression in interphase cells [24,25,45,46]. The other important difference is while the vinca alkaloids affect both microtubule growth and shortening [46,47], eribulin exerts its cytotoxicity effect only on microtubule growth with little or no effect on microtubule shortening [24,25,45,46]. Furthermore, eribulin showed a favorable side effect profile and tolerability with less peripheral neuropathy compared to other antimicrotubular targeted drugs in clinical trials [23,26,46].

Considering the important role of PARP3 in the mitotic pathway and centrosome function, we tested the effect of olaparib as a PARP3 inhibitor on eribulin cytotoxicity. Our results shed light on a new method of using PARP3 inhibitors with anti-microtubule agents. Based on our results, the drug combination of eribulin with a PARP3 inhibitor, olaparib demonstrated a significant reduction of IC_{50} values (3–7-fold) in all tested breast cancer cell lines including the TNBC cell lines (MDA-436, and MDA-231) and one ER+/HER2- breast cancer cell line, MCF-7. Preferential sensitization by olaparib in MDA cells with respect to MCF-7 cells might be associated with reduced HRR proficiency reported in MDA-436 and MDA-231 [48]. In fact, BRCA2, a component of HRR is mutated in MDA-436 cells. In contrast MDA-231 cells do not display mutated HRR genes but show enrichment of BRCAness score [49] that has been correlated with biologically aggressive TNBC tumors segregating with BRCA1/2 tumors in the absence of mutations in these genes [50]. This agrees with our findings showing that olaparib enhances eribulin-induced cytotoxicity in the BRCA2 deficient MDA-436 cells. Notably, PARP3 is necessary for efficient mitotic progression during mitosis and mitotic spindle dynamics [16–18,22]. In fact, we previously have shown that selective PARP3 inhibitors enhance vinorelbine cytotoxicity in breast cancer cell lines [22]. Also, in previous investigations, eribulin alone induced G2/M cell cycle phase arrest and abnormal mitosis and subsequent apoptosis followed by cell death [23,26,27]. Apoptotic cell death occurrence after G2/M phase cell cycle arrest has been previously demonstrated [34,47]. Eribulin exerts potent *in vitro* antitumor effects in breast cancer cells via mitotic spindle disruption compromising and interfering with cell division which leads to marked accumulation of cells in G2/M phase [25,29,51]. The PARP3 inhibitor, olaparib and eribulin drug combination enhanced eribulin induced G2/M phase accumulation and cell cycle arrest compared to eribulin alone as indicated by flow cytometry analysis.

Based on our results, eribulin or olaparib alone inhibited PARP3 activity, but the eribulin and olaparib drug combination reduced PARP3 activity significantly more than eribulin alone. In a similar fashion, the same significant reduction of PARP3 activity has been shown by us, using the olaparib and vinorelbine drug combination against TNBC [22].

During mitosis, microtubules undergo rapid polymerization and depolymerization to allow chromosome movement [52]. Effective bipolar spindle organization in the mitotic phase is highly regulated by centrosome duplication during each cell cycle of dividing cells [53]. Anti-microtubule targeting agents like eribulin bind tubulin and prevent its incorporation into growing microtubules leading to microtubule disassembly and increased splayed and defective tubulin via alteration of microtubule network and suppression of mitotic spindle dynamics [24,25,45]. As expected, eribulin experimentally arrests cells during mitotic metaphase leading to mitotic catastrophe and apoptosis [24,25,52,54].

Eribulin induced microtubule instability and defective mitotic spindle dynamics in treated breast cancer cells, resulting in mitotic arrest and subsequent abnormal mitotic divisions with a more compact, irregular spindle fiber appearance and increased chromosome misalignment [23,26,27,45]. Based on our results, these types of mitotic catastrophe effects are enhanced by the combination of eribulin with the PARP inhibitor, olaparib. Inhibition of PARP3 with olaparib potentiates eribulin-induced mitotic catastrophe due to microtubule network alterations, abnormal mitosis, and cell cycle arrest.

Interestingly, inhibition of PARP3 sensitizes breast cancer cells to vinorelbine and eribulin in spite of their different mechanisms of interacting with the tubulin structure but not to paclitaxel which interacts with tubulin in a different fashion then the above two anticancer agents.

In conclusion, the results of our current study should lead the way to new approaches for targeting HER2 negative metastatic breast cancer. However, combination of olaparib with vinorelbine or eribulin in clinical trials should be

done utilizing the known pharmacokinetics and toxicities of these drugs; i.e., specifically utilizing limited exposure time (5–7 days) of olaparib with every 2 week schedules of anticancer drugs to allow for the use of granulocyte stimulating agents to overcome increased myelotoxicity and maximize potentially synergistic antitumor activity. A previous phase II trial of olaparib given daily continuously and eribulin days 1 and 8 resulted in significant myelosuppression [55].

Availability of Data and Materials

Not applicable.

Author Contributions

BSA, LP and RA designed the research study. BSA performed the experimental work and data acquisition. BSA and RA analyzed and interpreted the results. All authors contributed to editorial changes in the manuscript. All authors read and approved the final manuscript.

Ethics Approval and Consent to Participate

Not applicable.

Acknowledgment

The authors acknowledge the Cancer Research Society.

Funding

Cancer Research Society (Montreal, Grant number 01713).

Conflict of Interest

The authors declare no conflict of interest.

Supplementary Material

Supplementary material associated with this article can be found, in the online version, at https://doi.org/10.31083/j.fbl2803052.

References

[1] De Vos M, Schreiber V, Dantzer F. The diverse roles and clinical relevance of PARPs in DNA damage repair: current state of the art. Biochemical Pharmacology. 2012; 84: 137–146.

[2] Sonnenblick A, de Azambuja E, Azim HA, Jr, Piccart M. An update on PARP inhibitors–moving to the adjuvant setting. Nature Reviews. Clinical Oncology. 2015; 12: 27–41.

[3] Robert M, Frenel JS, Gourmelon C, Patsouris A, Augereau P, Campone M. Olaparib for the treatment of breast cancer. Expert Opinion on Investigational Drugs. 2017; 26: 751–759.

[4] Tutt A, Robson M, Garber JE, Domchek SM, Audeh MW, Weitzel JN, *et al*. Oral poly(ADP-ribose) polymerase inhibitor olaparib in patients with BRCA1 or BRCA2 mutations and advanced breast cancer: a proof-of-concept trial. Lancet. 2010; 376: 235–244.

[5] Chan SL, Mok T. PARP inhibition in BRCA-mutated breast and ovarian cancers. Lancet. 2010; 376: 211–213.

[6] Arun B, Akar U, Gutierrez-Barrera AM, Hortobagyi GN, Ozpolat B. The PARP inhibitor AZD2281 (Olaparib) induces autophagy/mitophagy in BRCA1 and BRCA2 mutant breast cancer cells. International Journal of Oncology. 2015; 47: 262–268.

[7] Rizvi W, Truong P, Truong Q. Metastatic Breast Cancer with BRCA Mutation Discovered By Next-Generation Sequencing Responding to Olaparib. Cureus. 2017; 9: e1337.

[8] Dizdar O, Arslan C, Altundag K. Advances in PARP inhibitors for the treatment of breast cancer. Expert Opinion on Pharmacotherapy. 2015; 16: 2751–2758.

[9] Creeden JF, Nanavaty NS, Einloth KR, Gillman CE, Stanbery L, Hamouda DM, *et al*. Homologous recombination proficiency in ovarian and breast cancer patients. BMC Cancer. 2021; 21: 1154.

[10] D'Andrea AD. Mechanisms of PARP inhibitor sensitivity and resistance. DNA Repair. 2018; 71: 172–176.

[11] Zwetsloot AJ, Tut G, Straube A. Measuring microtubule dynamics. Essays in Biochemistry. 2018; 62: 725–735.

[12] Chen A. PARP inhibitors: its role in treatment of cancer. Chinese Journal of Cancer. 2011; 30: 463–471.

[13] Robson M, Im SA, Senkus E, Xu B, Domchek SM, Masuda N, *et al*. Olaparib for Metastatic Breast Cancer in Patients with a Germline BRCA Mutation. New England Journal of Medicine. 2017; 377: 523–533.

[14] Langelier MF, Riccio AA, Pascal JM. PARP-2 and PARP-3 are selectively activated by 5' phosphorylated DNA breaks through an allosteric regulatory mechanism shared with PARP-1. Nucleic Acids Research. 2014; 42: 7762–7775.

[15] Krishnakumar R, Kraus WL. The PARP side of the nucleus: molecular actions, physiological outcomes, and clinical targets. Molecular Cell. 2010; 39: 8–24.

[16] Boehler C, Gauthier LR, Mortusewicz O, Biard DS, Saliou JM, Bresson A, *et al*. Poly(ADP-ribose) polymerase 3 (PARP3), a newcomer in cellular response to DNA damage and mitotic progression. Proceedings of the National Academy of Sciences of the United States of America. 2011; 108: 2783–2788.

[17] Fernández-Marcelo T, Frías C, Pascua I, de Juan C, Head J, Gómez A, *et al*. Poly (ADP-ribose) polymerase 3 (PARP3), a potential repressor of telomerase activity. Journal of Experimental & Clinical Cancer Research. 2014; 33: 19.

[18] Augustin A, Spenlehauer C, Dumond H, Ménissier-De Murcia J, Piel M, Schmit AC, *et al*. PARP-3 localizes preferentially to the daughter centriole and interferes with the G1/S cell cycle progression. Journal of Cell Science. 2003; 116: 1551–1562.

[19] Boehler C, Dantzer F. PARP-3, a DNA-dependent PARP with emerging roles in double-strand break repair and mitotic progression. Cell Cycle. 2011; 10: 1023–1024.

[20] Robert I, Gaudot L, Rogier M, Heyer V, Noll A, Dantzer F, *et al*. Parp3 negatively regulates immunoglobulin class switch recombination. PLoS Genetics. 2015; 11: e1005240.

[21] Rulten SL, Fisher AEO, Robert I, Zuma MC, Rouleau M, Ju L, *et al*. PARP-3 and APLF function together to accelerate nonhomologous end-joining. Molecular Cell. 2011; 41: 33–45.

[22] Sharif-Askari B, Amrein L, Aloyz R, Panasci L. PARP3 inhibitors ME0328 and olaparib potentiate vinorelbine sensitization in breast cancer cell lines. Breast Cancer Research and Treatment. 2018; 172: 23–32.

[23] Swami U, Chaudhary I, Ghalib MH, Goel S. Eribulin – a review of preclinical and clinical studies. Critical Reviews in Oncology/hematology. 2012; 81: 163–184.

[24] Smith JA, Wilson L, Azarenko O, Zhu X, Lewis BM, Littlefield BA, *et al*. Eribulin binds at microtubule ends to a single site on tubulin to suppress dynamic instability. Biochemistry. 2010; 49: 1331–1337.

[25] Dybdal-Hargreaves NF, Risinger AL, Mooberry SL. Eribulin mesylate: mechanism of action of a unique microtubule-

targeting agent. Clinical Cancer Research. 2015; 21: 2445–2452.

[26] Shingaki S, Kogawa T, Shimokawa M, Harano K, Naito Y, Kusuhara S, *et al*. Use of eribulin as an earlier-line chemotherapy for patients with HER2-negative metastatic breast cancer. Journal of Cancer. 2020; 11: 4099–4105.

[27] Pizzuti L, Krasniqi E, Barchiesi G, Mazzotta M, Barba M, Amodio A, *et al*. Eribulin in Triple Negative Metastatic Breast Cancer: Critic Interpretation of Current Evidence and Projection for Future Scenarios. Journal of Cancer. 2019; 10: 5903–5914.

[28] Islam B, Lustberg M, Staff NP, Kolb N, Alberti P, Argyriou AA. Vinca alkaloids, thalidomide and eribulin-induced peripheral neurotoxicity: From pathogenesis to treatment. Journal of the Peripheral Nervous System. 2019; 24: S63–S73.

[29] Muñoz-Couselo E, Pérez-García J, Cortés J. Eribulin mesylate as a microtubule inhibitor for treatment of patients with metastatic breast cancer. OncoTargets and Therapy. 2011; 4: 185–192.

[30] Davidson D, Wang Y, Aloyz R, Panasci L. The PARP inhibitor ABT-888 synergizes irinotecan treatment of colon cancer cell lines. Investigational New Drugs. 2013; 31: 461–468.

[31] Vichai V, Kirtikara K. Sulforhodamine B colorimetric assay for cytotoxicity screening. Nature Protocols. 2006; 1: 1112–1116.

[32] Davidson D, Coulombe Y, Martinez-Marignac VL, Amrein L, Grenier J, Hodkinson K, *et al*. Irinotecan and DNA-PKcs inhibitors synergize in killing of colon cancer cells. Investigational New Drugs. 2012; 30: 1248–1256.

[33] Davidson D, Grenier J, Martinez-Marignac V, Amrein L, Shawi M, Tokars M, *et al*. Effects of the novel DNA dependent protein kinase inhibitor, IC486241, on the DNA damage response to doxorubicin and cisplatin in breast cancer cells. Investigational New Drugs. 2012; 30: 1736–1742.

[34] Xu ZY, Loignon M, Han FY, Panasci L, Aloyz R. Xrcc3 induces cisplatin resistance by stimulation of Rad51-related recombinational repair, S-phase checkpoint activation, and reduced apoptosis. The Journal of Pharmacology and Experimental Therapeutics. 2005; 314: 495–505.

[35] Blajeski AL, Phan VA, Kottke TJ, Kaufmann SH. G(1) and G(2) cell-cycle arrest following microtubule depolymerization in human breast cancer cells. The Journal of Clinical Investigation. 2002; 110: 91–99.

[36] Delgado M, Urbaniak A, Chambers TC. Contrasting effects of microtubule destabilizers versus stabilizers on induction of death in G1 phase of the cell cycle. Biochemical Pharmacology. 2019; 162: 213–223.

[37] Deng S, Krutilina RI, Wang Q, Lin Z, Parke DN, Playa HC. An Orally Available Tubulin Inhibitor, VERU-111, Suppresses Triple-Negative Breast Cancer Tumor Growth and Metastasis and Bypasses Taxane Resistance. Molecular Cancer Therapeutics. 2020; 19: 348–363.

[38] Diem K, Magaret A, Klock A, Jin L, Zhu J, Corey L. Image analysis for accurately counting CD4+ and CD8+ T cells in human tissue. Journal of Virological Methods. 2015; 222: 117–121.

[39] Towle MJ, Salvato KA, Budrow J, Wels BF, Kuznetsov G, Aalfs KK, *et al*. In vitro and in vivo anticancer activities of synthetic macrocyclic ketone analogues of halichondrin B. Cancer Research. 2001; 61: 1013–1021.

[40] Benlloch R, Castejón R, Rosado S, Coronado MJ, Sánchez P, Romero J. In vitro radiosensitization by eribulin in human cancer cell lines. Reports of Practical Oncology and Radiotherapy. 2022; 27: 509–518.

[41] Akoumianaki T, Kardassis D, Polioudaki H, Georgatos SD, Theodoropoulos PA. Nucleocytoplasmic shuttling of soluble tubulin in mammalian cells. Journal of Cell Science. 2009; 122: 1111–1118.

[42] Curtin NJ, Szabo C. Therapeutic applications of PARP inhibitors: anticancer therapy and beyond. Molecular Aspects of Medicine. 2013; 34: 1217–1256.

[43] Meng XW, Koh BD, Zhang JS, Flatten KS, Schneider PA, Billadeau DD, *et al*. Poly(ADP-ribose) polymerase inhibitors sensitize cancer cells to death receptor-mediated apoptosis by enhancing death receptor expression. The Journal of Biological Chemistry. 2014; 289: 20543–20558.

[44] Pettitt SJ, Lord CJ. Dissecting PARP inhibitor resistance with functional genomics. Current Opinion in Genetics & Development. 2019; 54: 55–63.

[45] Okouneva T, Azarenko O, Wilson L, Littlefield BA, Jordan MA. Inhibition of centromere dynamics by eribulin (E7389) during mitotic metaphase. Molecular Cancer Therapeutics. 2008; 7: 2003–2011.

[46] Jain S, Cigler T. Eribulin mesylate in the treatment of metastatic breast cancer. Biologics: Targets & Therapy. 2012; 6: 21–29.

[47] Jordan MA, Wilson L. Microtubules as a target for anticancer drugs. Nature Reviews. Cancer. 2004; 4: 253–265.

[48] Peng G, Chun-Jen Lin C, Mo W, Dai H, Park YY, Kim SM, *et al*. Genome-wide transcriptome profiling of homologous recombination DNA repair. Nature Communications. 2014; 5: 3361.

[49] Oshi M, Gandhi S, Wu R, Asaoka M, Yan L, Yamada A, *et al*. Development of a novel BRCAness score that predicts response to PARP inhibitors. Biomarker Research. 2022; 10: 80.

[50] Palacios J, Honrado E, Osorio A, Cazorla A, Sarrió D, Barroso A, *et al*. Immunohistochemical characteristics defined by tissue microarray of hereditary breast cancer not attributable to BRCA1 or BRCA2 mutations: differences from breast carcinomas arising in BRCA1 and BRCA2 mutation carriers. Clinical Cancer Research. 2003; 9: 3606–3614.

[51] Tsuda Y, Iimori M, Nakashima Y, Nakanishi R, Ando K, Ohgaki K, *et al*. Mitotic slippage and the subsequent cell fates after inhibition of Aurora B during tubulin-binding agent-induced mitotic arrest. Scientific Reports. 2017; 7: 16762.

[52] Goodson HV, Jonasson EM. Microtubules and Microtubule-Associated Proteins. Cold Spring Harbor Perspectives in Biology. 2018; 10: a022608.

[53] Fujita H, Yoshino Y, Chiba N. Regulation of the centrosome cycle. Molecular & Cellular Oncology. 2015; 3: e1075643.

[54] Wang YR, Xu Y, Jiang ZZ, Guerram M, Wang B, Zhu X, *et al*. Deoxypodophyllotoxin induces G2/M cell cycle arrest and apoptosis in SGC-7901 cells and inhibits tumor growth in vivo. Molecules. 2015; 20: 1661–1675.

[55] Yonemori K, Shimomura A, Yasojima H, Masuda N, Aogi K, Takahashi M, *et al*. A phase I/II trial of olaparib tablet in combination with eribulin in Japanese patients with advanced or metastatic triple-negative breast cancer previously treated with anthracyclines and taxanes. European Journal of Cancer. 2019; 109: 84–91.